

Tian Ho Seah¹ and Teerawut Juirnarongrit²

Constant Rate of Strain Consolidation with Radial Drainage

ABSTRACT: This paper describes a method of determining the consolidation characteristics of soft Bangkok clay under the radial drainage condition by using a newly developed constant rate of strain (CRS) consolidometer. A new formulation for this type of test was proposed. A series of constant rate-of-strain consolidation tests were compared to the results of oedometer tests. The pore water pressure distribution across the specimen in the CRS tests was estimated from measurements made at two locations. The results agreed well with the theoretical solution. A simple method of estimating the preconsolidation pressure by means of the pore water pressure ratio is also proposed. Because the tests conducted at different strain rates indicate that apparent preconsolidation pressure increases with strain rate, it is believed that secondary compression occurred during primary consolidation for this clay. The consolidation characteristics, including coefficient of consolidation and coefficient of permeability, in the vertical and horizontal directions were also compared.

KEYWORDS: anisotropy, clays, consolidation, laboratory tests, permeability, time dependence

Notation

α	Constant
A	Area
β	Constant
c	Coefficient of consolidation
$C_{\alpha c}$	Coefficient 1 of secondary compression
C_c	Compression Index
c_h	Horizontal coefficient of consolidation
CR	Compression ratio
c_v	Vertical coefficient of consolidation
$\dot{\epsilon}$	Strain rate (s)
ϵ_v	Vertical strain (%)
e	Base of natural logarithm = 2.718
e	Void ratio
e_{op}	End of primary consolidation
H	Vertical drainage path
i	Hydraulic gradient
γ_w	Unit weight of water (kN/m ³)
k	Coefficient of permeability (cm/s)
k_h	Horizontal coefficient of permeability (cm/s)
k_v	Vertical coefficient of permeability (cm/s)
m_v	Coefficient of volume compressibility (1/kPa)
n	r_e/r_w = ratio of radius of specimen to radius of central drain
q	Discharge of water
r	Distance from center of cylindrical specimen
r_e	Radius of specimen
r_w	Radius of central drain
T_h	Time factor for radial flow = $\frac{c_h t}{4r_e^2}$
T_v	Time factor for vertical flow

t	Time (s)
\bar{u}	Average excess pore pressure across specimen (kPa)
u	Pore water pressure (kPa)
u_o	Initial excess pore pressure (kPa)
u_a	Excess pore water pressure at 13 mm from center of specimen (kPa)
u_b	Excess pore water pressure at outer boundary (kPa)
u/u_b	Excess pore pressure ratio
u_b/σ_v	Pore pressure ratio
v_p	Velocity of piston (mm/s)

Introduction

For most sedimentary clay, the coefficient of consolidation in the horizontal direction (c_h) is usually different from the coefficient of consolidation in the vertical direction (c_v) due to the anisotropic nature of soil. The coefficient of consolidation is commonly determined with the one-dimensional oedometer test; however, measurements are limited to the vertical direction only. The design of some field applications, such as ground improvement using prefabricated vertical drains (PVD), requires soil properties in both directions. In recent years, PVD have been used extensively in Thailand and throughout Southeast Asia. The Rowe cell (Rowe and Bardon 1966) with radial drainage is sometimes used to obtain horizontal consolidation parameters since water can flow in the radial direction under vertical loading, which simulates field conditions. This stress-controlled test is usually conducted with a load increment ratio of 1. However, results may produce poor consolidation curves in sensitive clays. In addition, the test is relatively time consuming to conduct and interpret. Therefore, the constant rate of strain (CRS) consolidometer with radial drainage (Fig. 1) was developed to alleviate some of those limitations.

The scope of the work includes formulation of new equations for constant rate of strain consolidation of saturated soil under radial drainage conditions. Soft Bangkok clay was used in testing, and the results were compared with conventional oedometer tests as well as other field measurements.

Received December 6, 2000; accepted for publication November 15, 2002; published November 17, 2003.

¹ Geotechnical Engineer, MAA Geotechnics Company, 39/165-7 Mu 13 Lad Phrao Road, Bangkok 10230, Thailand.

² Former graduate student of the Asian Institute of Technology, MAA Geotechnics Company, 39/165-7 Mu 13 Lad Phrao Road, Bangkok 10230, Thailand.

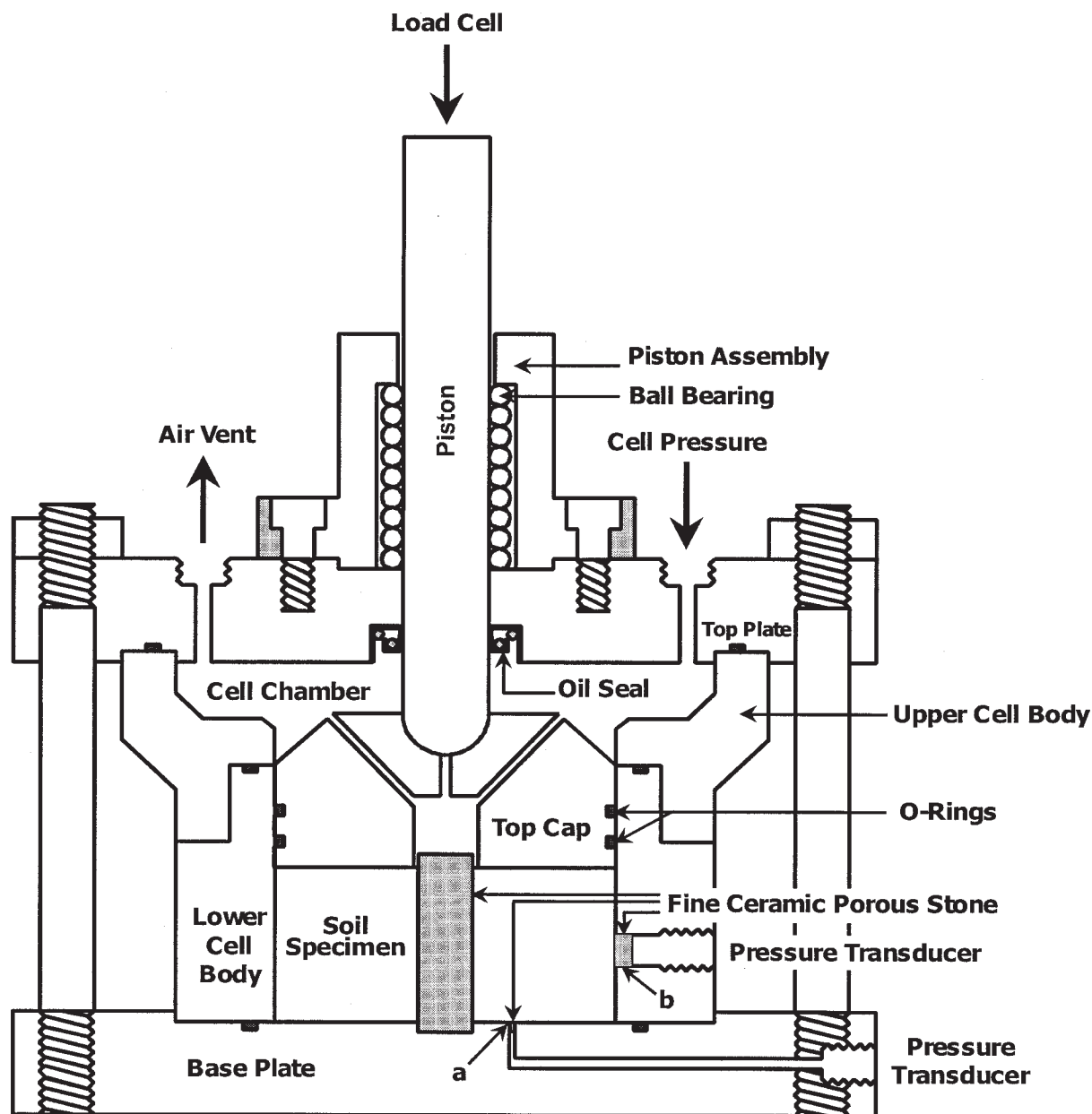


FIG. 1—Schematic diagram of CRS consolidometer with radial drainage.

Formulation

Barron (1948) conducted a comprehensive study of consolidation with radial flow by making assumptions similar to Terzaghi's one-dimensional consolidation theory except that water flow was considered to be in the horizontal direction. Two types of vertical boundary conditions were considered by Barron: (1) "free vertical strain" resulting from a uniform distribution of surface load, and (2) "equal vertical strain" resulting from imposing the same vertical deformation at all points on the surface. The differential equation can be written as

$$c_h \left(\frac{\partial^2 u}{\partial r^2} + \frac{1}{r} \frac{\partial u}{\partial r} \right) = \frac{\partial u}{\partial t} \tag{1}$$

where

u = the pore water pressure, and
 r = the distance from center of cylindrical specimen.

The solution under ideal conditions (no smear and no well resistance) for equal strain using a rigid top cap in a CRS test with a central drain is as follows:

$$u = \frac{\bar{u}}{r_e^2 \cdot F(n)} [r_e^2 \ln(r/r_w) - (r^2 - r_w^2)/2] = B[r_e^2 \ln(r/r_w) - (r^2 - r_w^2)/2] \tag{2}$$

where

$$\bar{u} = u_o e^\lambda, \lambda = -\frac{8T_h}{F(n)} \text{ and } F(n) = \frac{n^2}{n^2 - 1} \ln(n) - \frac{3n^2 - 1}{4n^2}$$

where

- \bar{u} = the average excess pore pressure across specimen,
- u_o = the initial excess pore pressure,
- r_e = the radius of specimen,
- r_w = the radius of central drain, and
- n = the ratio of radius of specimen to radius of central drain.

The following assumptions are used to solve the equations for the CRS test with radial flow:

1. Soil is homogeneous and isotropic.
2. Soil is fully saturated.
3. Soil deforms uniformly in the vertical direction only; hence, the effective stress is constant throughout the specimen.
4. Water and soil particles are incompressible.
5. Darcy's law is valid.
6. The effect of soil smear near the well boundary and the flow resistance within the well itself are both neglected.

7. Water only dissipates from the soil radially.
8. Soil deformations are small; therefore, the small strain theory applies.

Equations formulated for this CRS consolidation test are used to calculate following parameters:

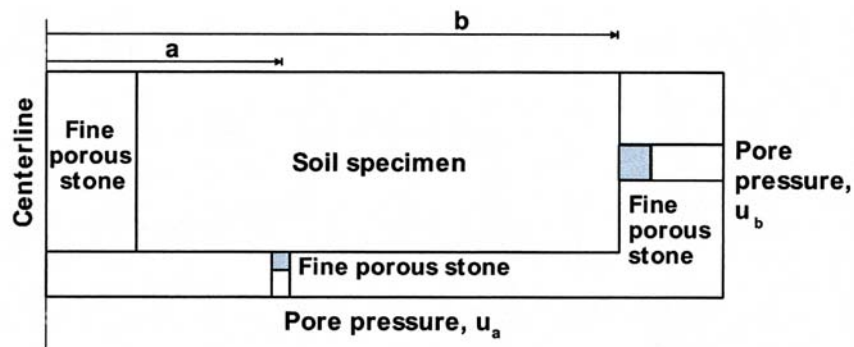
1. Horizontal coefficient of permeability (k_h).
2. Horizontal coefficient of consolidation (c_h).
3. Effective vertical stress (σ'_v).

Figure 2 shows the pore pressure distribution based on Barron's theory for equal vertical strain. By applying boundary conditions of $r = r_e$ and $u = u_b$, then

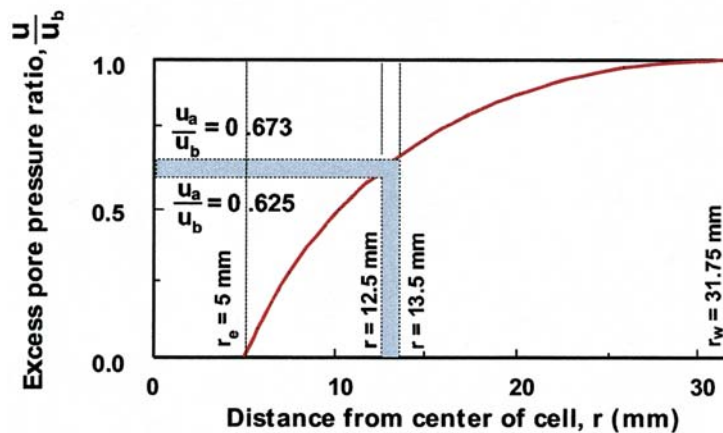
$$B = \frac{u_b}{[r_e^2 \ln(r_e/r_w) - (r_e^2 - r_w^2)/2]} \quad (3)$$

Differentiating Eq 2 with respect to r gives:

$$\frac{\partial u}{\partial r} = B(r_e^2/r - r) = B \cdot (r_e^2 - r^2)/r \quad (4)$$



a) Locations of pore water pressure measurement



b) Excess pore pressure ratio versus radius

FIG. 2—Pore water pressure distribution.

Based on Darcy's law, the discharge of water, q , can be written as

$$q = k i A$$

$$q = k_h \frac{dh}{dr} \left[2\pi \left(r + \frac{dr}{2} \right) H \right] = \frac{k_h}{\gamma_w} \frac{du}{dr} 2\pi r H \quad (5)$$

where

i = the hydraulic gradient, and
 H = the vertical drainage path.

Substituting Eq 4 into Eq 5 gives

$$q = \frac{2\pi k_h B H (r_e^2 - r_w^2)}{\gamma_w} \quad (6)$$

At $r = r_w$, discharge of water can be written as

$$q = \frac{2\pi k_h B H (r_e^2 - r_w^2)}{\gamma_w} \quad (7)$$

The discharge of water can also be expressed in terms of velocity of piston, v_p , as

$$q = v_p \cdot \pi (r_e^2 - r_w^2) \quad (8)$$

Equating Eqs 7 and 8 gives

$$k_h = \frac{v_p \cdot \gamma_w}{2BH} = \frac{v_p \cdot \gamma_w [r_e^2 \ln(r_e/r_w) - (r_e^2 - r_w^2)/2]}{2u_b H}$$

or

$$k_h = \alpha \frac{v_p \gamma_w r_e^2}{u_b H} \quad (9)$$

In this case, $r_w = 5.0$ mm and $r_e = 31.75$ mm, then $\alpha = 0.680$ as presented in Fig. 3.

The horizontal coefficient of consolidation is, therefore, given by:

$$c_h = \frac{k_h}{m_v \gamma_w} = \frac{\alpha v_p r_e^2}{u_b H m_v} \quad (10)$$

where m_v is the coefficient of volume compressibility

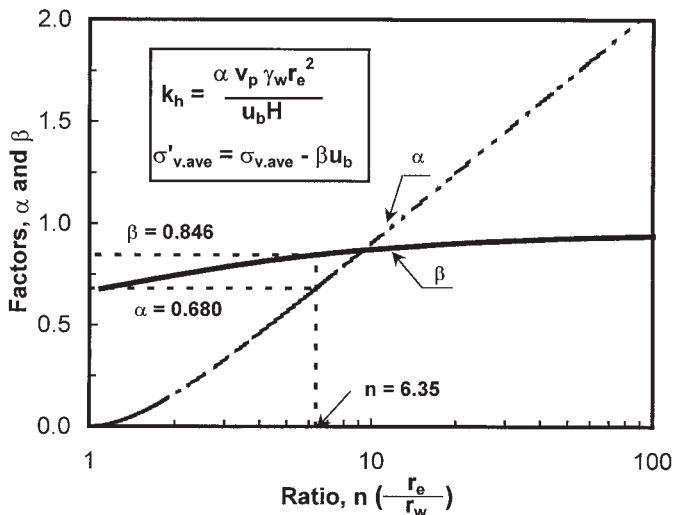


FIG. 3—Relationship among α , β , and n .

If the soil element deforms in the vertical direction only without any lateral movement, then the effective vertical stress will be constant throughout the specimen. The average effective vertical stress can be expressed as:

$$\sigma'_{v,ave} = \sigma_{v,ave} - \bar{u} \text{ or}$$

$$\sigma'_{v,ave} = \frac{P}{A} - \beta u_b \quad (11)$$

The factor, β , is given by

$$\beta = \frac{\int_{r_w}^{r_e} 2 \pi r u dr}{u_b A}$$

$$\beta = \frac{\left[r_e^4 \ln\left(\frac{r_e}{r_w}\right) - \frac{3r_e^4}{4} + r_w^2 r_e^2 - \frac{r_w^4}{4} \right]}{u_b A} \quad (12)$$

If $r_w = 5.0$ mm and $r_e = 31.75$ mm, then $\beta = 0.846$ (refer to Fig. 3).

Test Equipment and Procedures

The major components of the new CRS consolidometer consist of a base plate, upper and lower cell body, top plate, top cap, and a loading piston. A soil specimen is trimmed by a 63.5-mm inner-diameter cutting ring that is used as the specimen holder and is placed on the lower cell body. A hole in the middle of the soil is made by inserting a piece of piano wire through the center with guiding plates at both ends of the trimmed soil specimen. The wire is rotated around the guided holes of the plates until the soil in the middle hole is detached. The excess soil at the two ends is trimmed using the wire saw to give smooth surfaces. A cylindrical porous stone is then gently inserted in the cut hole, which will be used as the only drainage boundary of the soil specimen during consolidation. After trimming is completed, the lower cell body is fixed to the base plate with a 1-mm-diameter hole located 13 mm from the center (Location a). This small hole is filled with a fine porous stone at one end and connected to a pressure transducer at the other end. Pore water pressure is measured at the outer boundary with another pressure transducer (Location b) attached to the wall of the lower cell body. Excess pore pressure distributions within the specimen can be made using these two pore pressure measurements. The upper cell body acts as a water chamber to assist in specimen saturation. The top cap transfers load from the piston to the soil specimen. A 10-mm-diameter hole with a depth of 15 mm at the center of the top cap allows the cylindrical porous stone to slide freely during consolidation. Two greased o-rings on the top cap are used to prevent leakage through the gap between the top cap and cell body. Previously measured friction induced by the o-rings is deducted from the vertical force measurement to provide an estimate of the vertical load on the soil specimen. Two holes connected to the center of the top cap provide drainage.

Once the equipment is assembled, a backpressure of 200 kPa is applied to the soil specimen for saturation over a period of 24 h. The soil is loaded by a gear-driven loading frame that forces the loading piston to move downwards at a constant speed. The vertical load, pore water pressures, and displacement are measured

TABLE 1—General soil properties.

Depth (m)	Natural Water Content (%)	Total Unit Weight (kN/m ³)	Liquid Limit (%)	Plasticity Index (%)	Specific Gravity	Gradation (%)			Remarks
						Sand	Silt	Clay (<5 μm)	
2.5	85.8	14.4	95	67	2.70	4	28	68	Influence by water table
3.5	93.3	14.4	117	77	2.69	2	29	69	
4.5	92.1	14.5	109	74	2.66	2	23	75	Relatively uniform
5.5	86.9	14.5	92	63	2.67	13	20	67	
6.5	68.5	15.3	72	49	2.68	2	24	74	Presence of some sand seams

with a load cell, pressure transducers, and displacement transducer and are recorded automatically by a data acquisition system.

Material Tested and Testing Program

Bangkok clay from the Asian Institute of Technology (AIT) campus was used as the testing material. This soft clay in the Chao Phraya plain extends from 200 to 250 km in the East-West direction and 250 to 300 km in the North-South direction. The thickness at AIT is only about 8 m compared with a thickness of about 12 m in the Bangkok City area. Undisturbed samples were collected by using 1-m-long thin-walled piston samplers with 75-mm diameter from a depth of 3 to 6 m, with general soil properties given in Table 1.

Two series of consolidation tests were performed on the undisturbed samples of soft clay. The first series consists of CRS consolidation tests at different strain rates and the second series were conventional oedometer tests. The CRS consolidation tests were performed on samples from depths of 3.5 to 6.5 m with four different strain rates ranging from $0.3 \times 10^{-6}/s$ to $5 \times 10^{-6}/s$. The conventional oedometer tests were conducted as reference tests for comparison with the results of CRS tests.

Test Results and Discussion

The CRS test results include: (1) consistency tests, (2) effect of strain rate, (3) pore pressure distribution across the specimen with measurement at Location *a* (13 mm from the center of soil specimen) and Location *b* (the outer boundary of soil specimen), (4) a new method of determining preconsolidation pressure, and (5) a method to evaluate the anisotropic consolidation behavior.

Consistency of Results

Figure 4 presents the compression curves of three CRS tests performed on soil specimens at a $1 \times 10^{-6}/s$ strain rate under similar testing conditions. The compression curves of these tests are almost identical, indicating good repeatability and consistency. The CRS curves are also in close agreement with oedometer tests.

Other Test Results

The compression curves of specimens at a depth of 4.5 m with various strain rates are shown in Fig. 5, indicating a shift in compression curve to the right with increasing strain rate. Figure 6 presents the relationship of coefficient of consolidation (*c*) versus effective vertical stress conducted at different strain rates, showing that the *c* values in the over-consolidated range are much higher

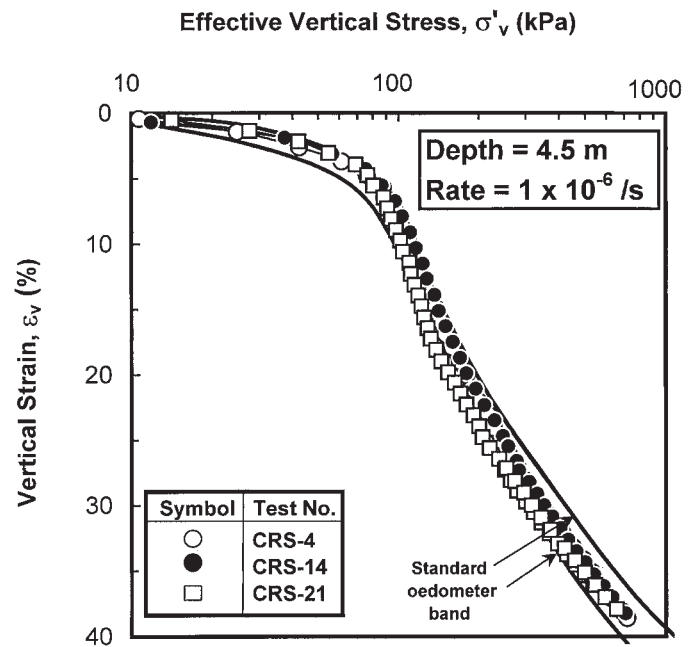


FIG. 4—Comparison between CRS and oedometer results.

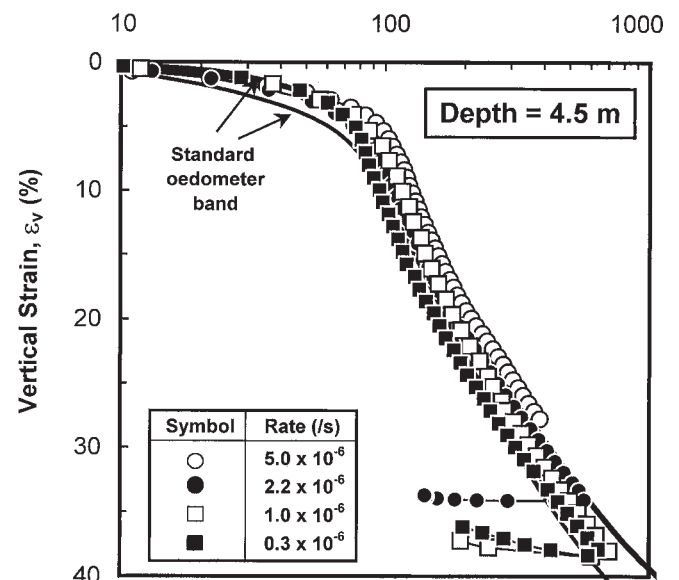


FIG. 5—Compression curves for different rates of strain.

than those in the normally consolidated range. An abrupt change occurred close to the preconsolidation pressure. But the results indicated that the horizontal coefficient of consolidation is independent of the strain rate. At any given stress, the vertical coefficient of consolidation from oedometer tests is less than the horizontal coefficient of consolidation. The horizontal coefficients of permeability from the CRS tests and the vertical coefficients of permeability from oedometer tests are plotted in Fig. 7. Although the k_h values decrease gradually in the overconsolidation range, they de-

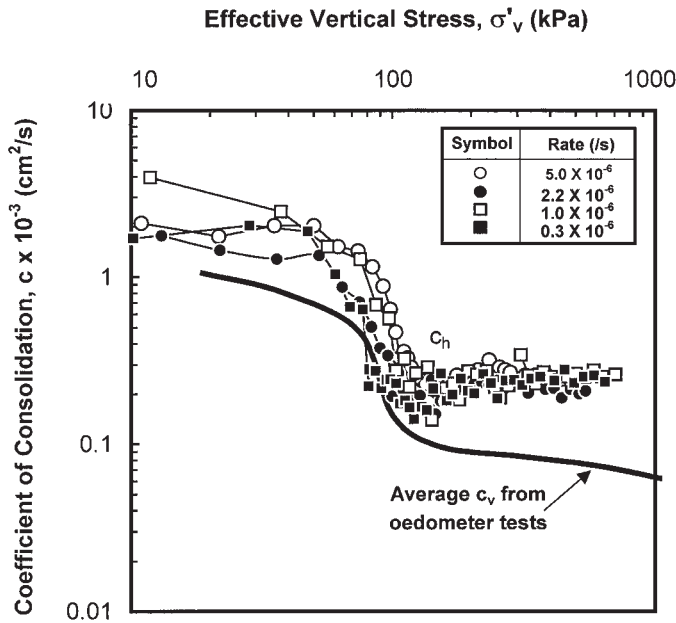


FIG. 6—Relationship between coefficient of consolidation and effective vertical stress.

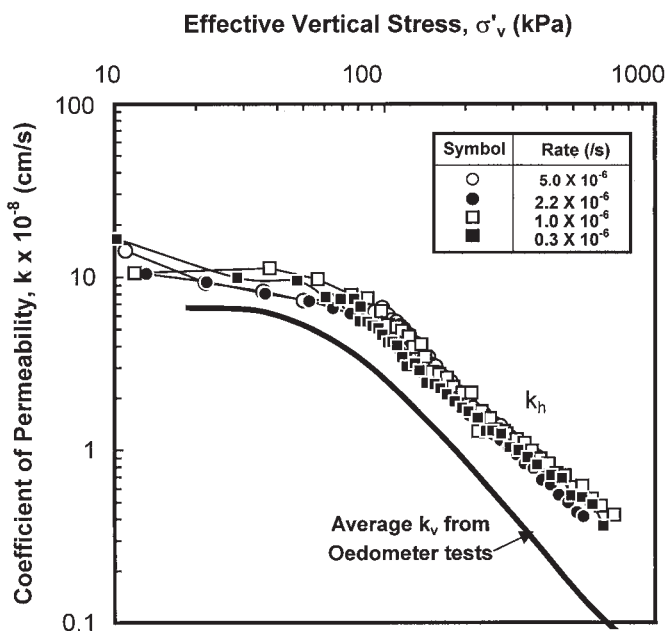


FIG. 7—Relationship between coefficient of permeability and effective vertical stress.

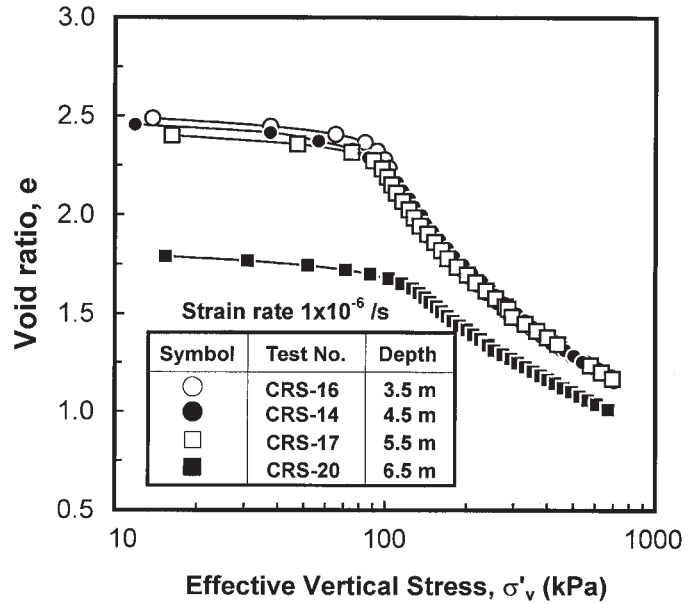


FIG. 8—Compression curves at depths of 3.5 to 6.5 m.

crease much more rapidly in the normal consolidation range due to larger changes in void ratios. The k_h is also independent of strain rate because the four k_h curves are similar.

To illustrate the consolidation characteristics of this soft clay layer, the compression curves of soil specimens collected between 3.5 and 6.5 m are plotted in Fig. 8.

Pore Water Pressure Distribution

The pore water pressures were measured at two locations as mentioned earlier, enabling the distribution of pore water pressure across the specimen to be known. Using Barron's theory, the excess pore water pressure ratio of u_a to u_b (see Fig. 2) is computed to be between 0.625 and 0.673. The pore pressure ratio versus effective vertical stress for various CRS tests are plotted as shown in Fig. 9a and 9b, indicating that the ratios are close to the theoretical values at low stress level. The pore pressure ratio at preconsolidation pressure as shown in Fig. 10 falls close to the theoretical band regardless of the strain rate, implying that the pore water pressure distribution across the specimen at small strain rate range can be represented by the solution proposed by Barron.

By defining a term, γ , as a function of c_h , specimen radius and pore pressure ratio, a plot of γ versus strain rate is given in Fig. 11, showing a linear relationship. For a given c_h value and specimen radius, the results indicated that the pore pressure ratio increases linearly with strain rate.

New Method of Determining Preconsolidation Pressure

Several methods exist for determining the preconsolidation pressure, such as Casagrande construction (1936), Schmertmann construction (1955), strain energy method (Tavenas et al. 1979), Janbu construction (1979), and Butterfield method (1979). All these methods require some form of construction and human judgment. From the CRS test results, it is observed that an alternative method of determining the preconsolidation pressure can be made from the plot of pore pressure ratio (u_b/σ_v) versus ef-

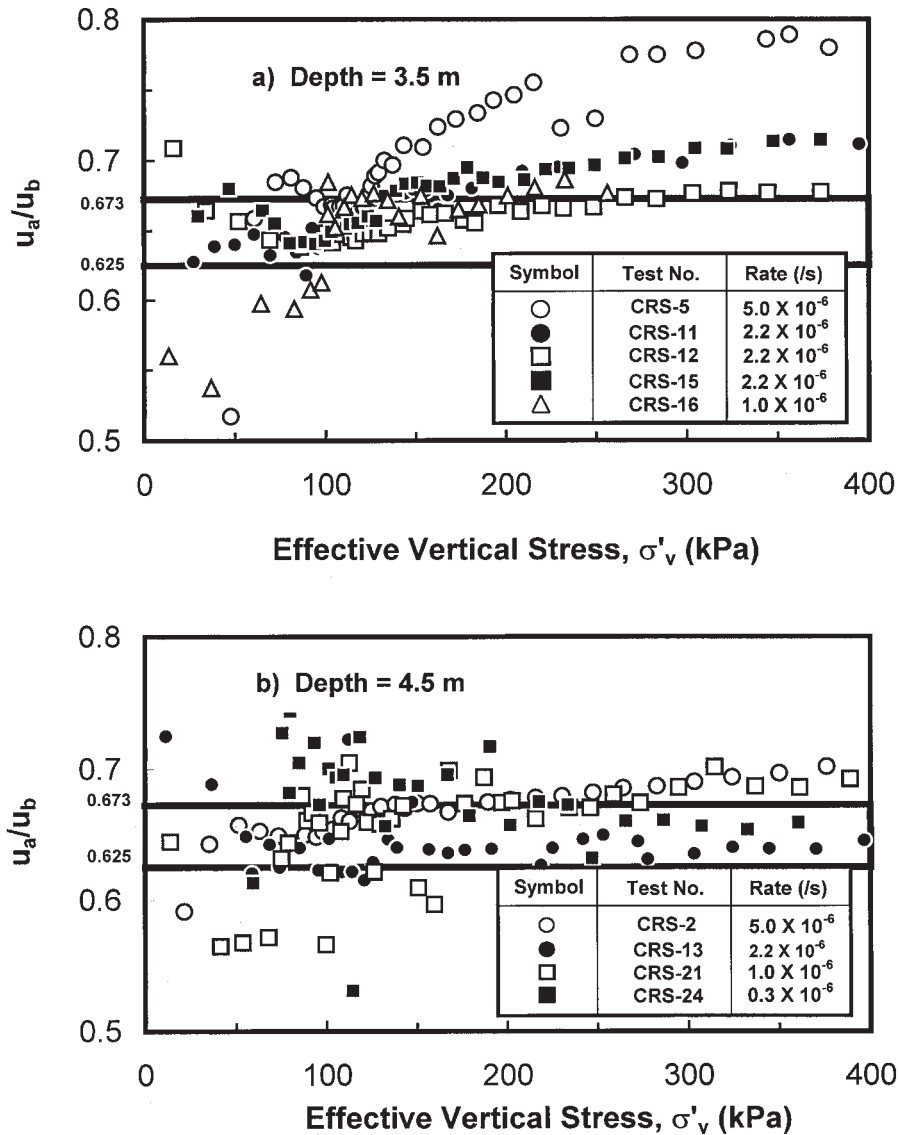


FIG. 9—Relationship between excess pore pressure ratio and effective vertical stress.

ffective vertical stress. Figure 12 shows the pore pressure ratio versus effective vertical stress, indicating a minimum stress ratio at the vicinity close to the preconsolidation pressure. Based on 23 CRS tests, the pressure at this minimum point seems to agree with the preconsolidation pressure obtained from Casagrande construction as shown in Fig. 13. The proposed method in determining preconsolidation pressure is much easier than traditional procedures.

Strain Rate Effect on Preconsolidation Pressure

As indicated in Fig. 5, the apparent preconsolidation pressure appears to be increased with strain rate. This phenomenon has been described by Ladd et al. (1977) as Hypotheses A and B in consolidation behavior. Hypothesis A assumes that creep occurs only after primary consolidation and consequently field compression will be similar to the laboratory curve. Whereas Hypothesis B assumes that deformation resulting from structural viscosity occurs during

pore water pressure dissipation and therefore strain at the end of primary consolidation increases with specimen thickness. Leroueil et al. (1988) devised a procedure to test the validity of the hypothesis by using a constant rate of strain test. If the compression curve is unique with different strain rates, i.e., the preconsolidation pressure remains the same, then Hypothesis A is valid. However, if different compression curves are obtained at different strain rates, then the preconsolidation pressure increases with increasing strain rate and Hypothesis B would be valid.

A plot of preconsolidation pressure versus strain rate is presented in Fig. 14, showing that the preconsolidation pressure increases linearly with increasing strain rate for all 23 specimens from various depths. The estimated strain rate at the end of primary consolidation in the oedometer based on an equation proposed by Leroueil (1988) is:

$$\dot{\epsilon} = \frac{0.434}{t_{eop}} \frac{C_{ae}}{C_c} \frac{C_c}{1 + e_o} = \frac{0.434}{T_{veop}} \frac{c_v}{H^2} \frac{C_{ae}}{C_c} CR \quad (13)$$

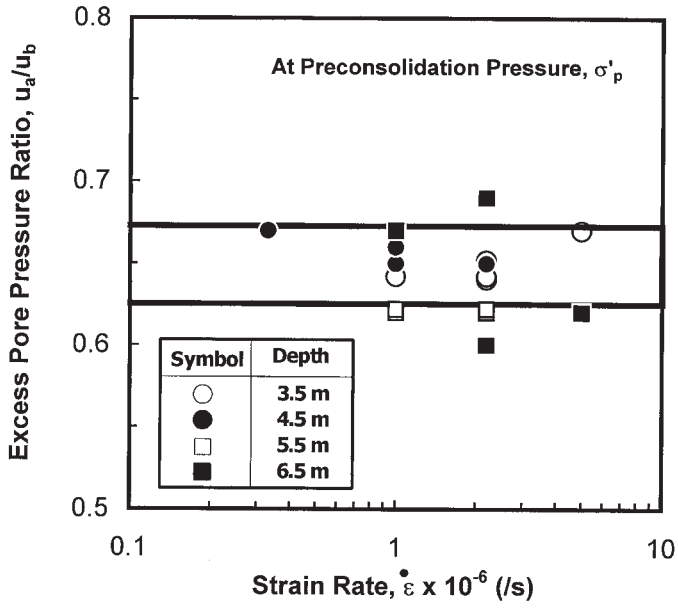


FIG. 10—Excess pore pressure ratios at preconsolidation pressure.

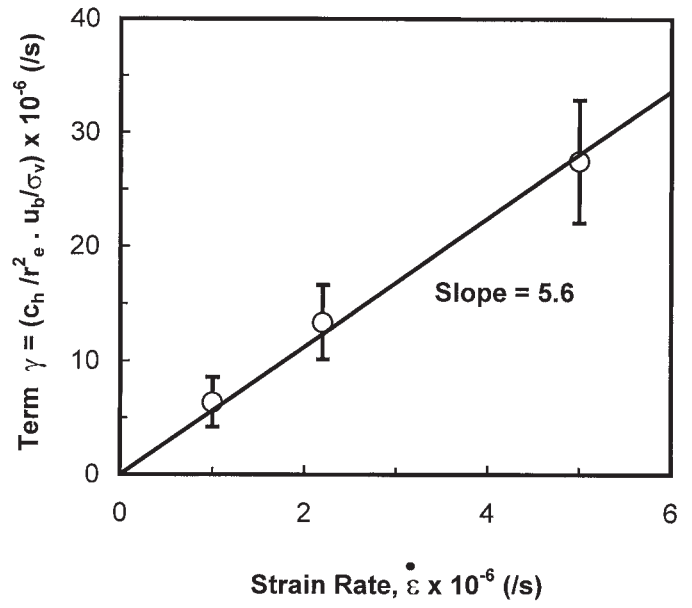


FIG. 11—Relationship between γ and strain rate.

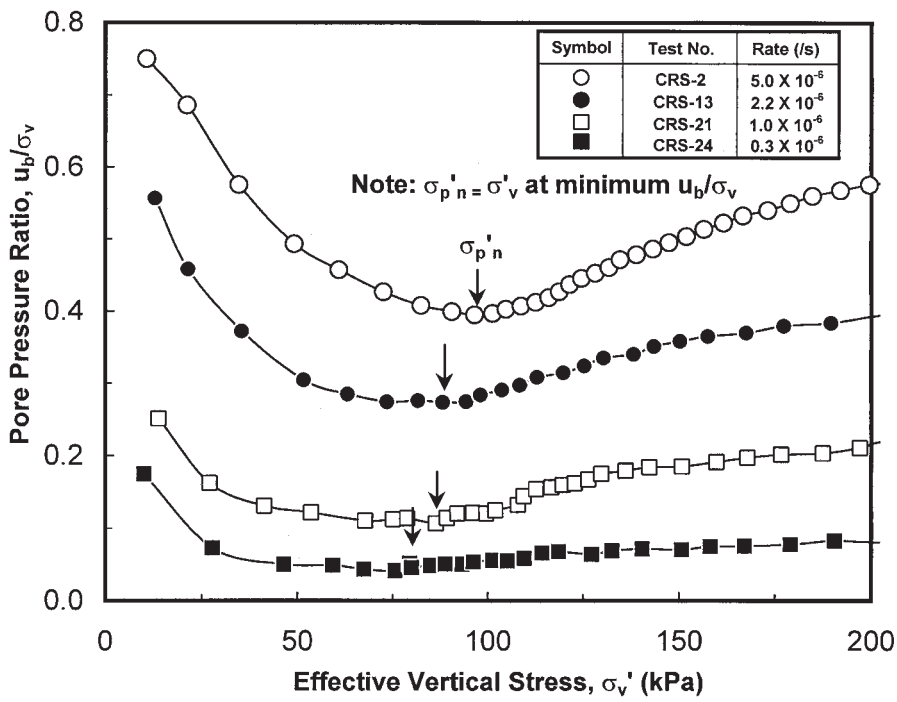


FIG. 12—Effective stress at minimum pore pressure ratio.

where

- C_c = the Compression Index,
- $C_{\alpha e}$ = the coefficient of secondary compression,
- c_v = the vertical coefficient of consolidation,
- CR = the compression ratio,
- e_o = the initial void ratio,
- $T_{v eop}$ = the time factor at the end of primary consolidation, and
- t_{eop} = the time at the end of primary consolidation.

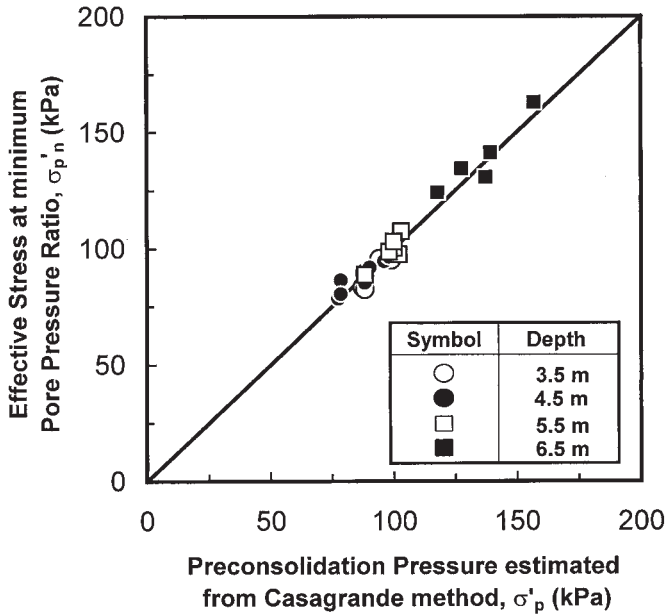


FIG. 13—New method of determining preconsolidation pressure.

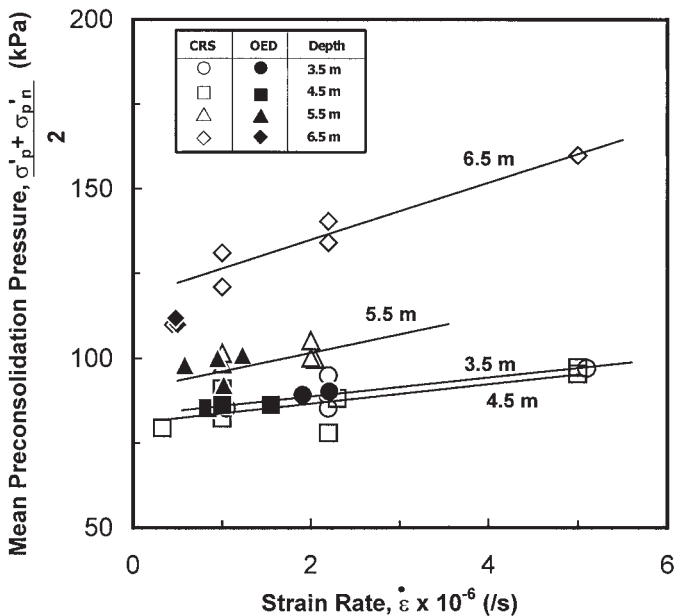


FIG. 14—Preconsolidation pressure versus strain rate.

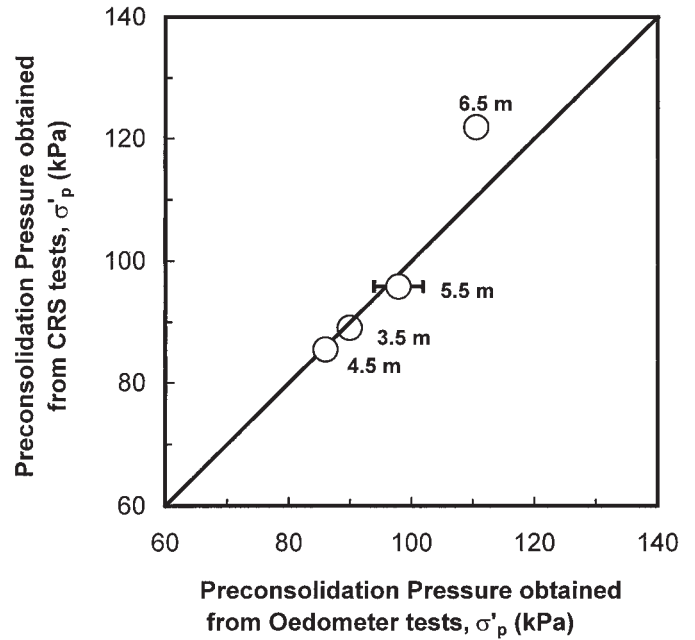


FIG. 15—Preconsolidation pressure obtained from different equipment.

Assuming the degree of primary consolidation is 99%, the corresponding time factor, $T_{v eop}$, is 1.78. If the $C_{\alpha e}/C_c$ value for Bangkok clay is assumed to be 0.04, then the estimated strain rate of oedometer tests at preconsolidation pressure ranges from 0.4×10^{-6} to 2×10^{-6} /s. The results from the oedometer tests are plotted along with the CRS tests in Fig. 14, indicating clearly the effect of strain rate on the preconsolidation pressure. Based on the linear relationship of preconsolidation pressure versus strain rate from the CRS tests, the preconsolidation pressures of the CRS tests at the same strain rate as in oedometer tests are compared with the results of oedometer tests shown in Fig. 15, indicating very good agreement.

Ratio of Horizontal to Vertical Coefficients of Consolidation

Based on the results from CRS and oedometer tests, plots of the ratio of horizontal to vertical coefficients of consolidation versus effective vertical stress for two depths are presented in Fig. 16. Anisotropy increases from 1.5 to 3 with increase in effective vertical stress from 20 to 500 kPa. At the effective overburden stress, the horizontal coefficient of consolidation is about 1.45 times higher than the vertical coefficient of consolidation (Fig. 17).

Ratio of Horizontal to Vertical Coefficients of Permeability

The results of horizontal and vertical coefficients of permeability are also compared (Fig. 18). The k_h/k_v ratio increases from 1.5 at stresses of 20 kPa to about 3.5 at 500 kPa. The horizontal coefficient of permeability at the effective overburden stress is also compared with the vertical coefficient of permeability in Fig. 19. The k_h/k_v ratio is 1.45, which should be equal to the c_h/c_v ratio.

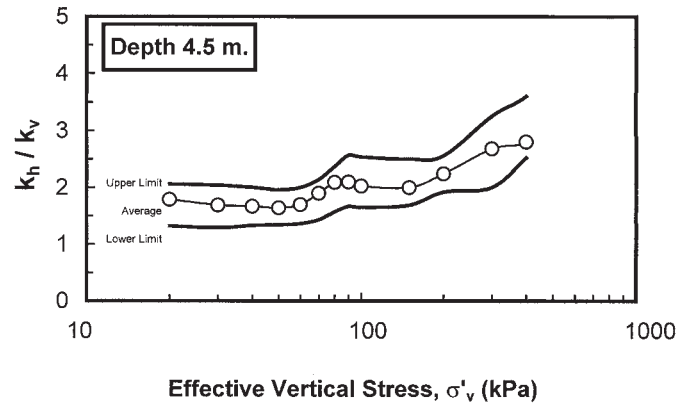
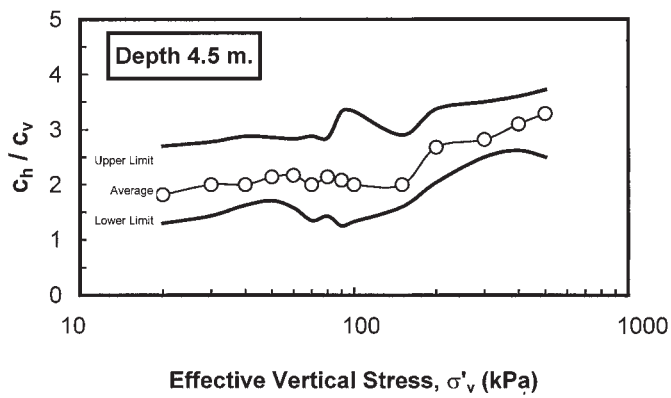
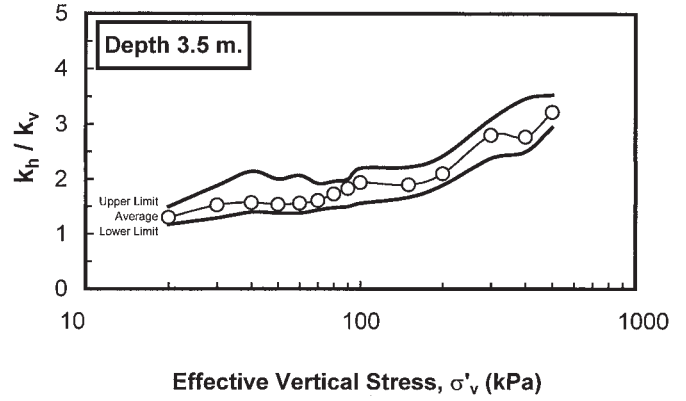
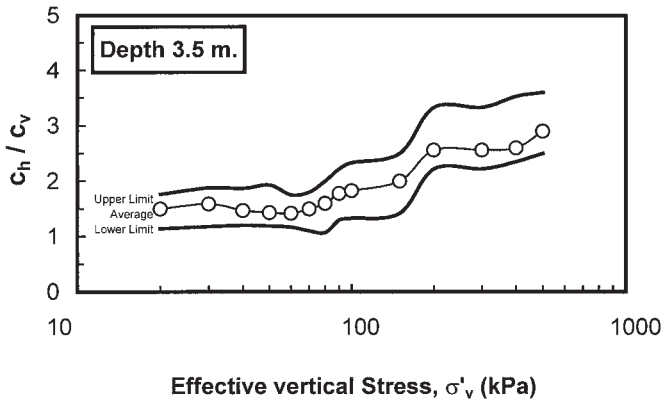


FIG. 16—Ratio of c_h/c_v versus effective vertical stress.

FIG. 18—Ratio of k_h/k_v versus effective vertical stress.

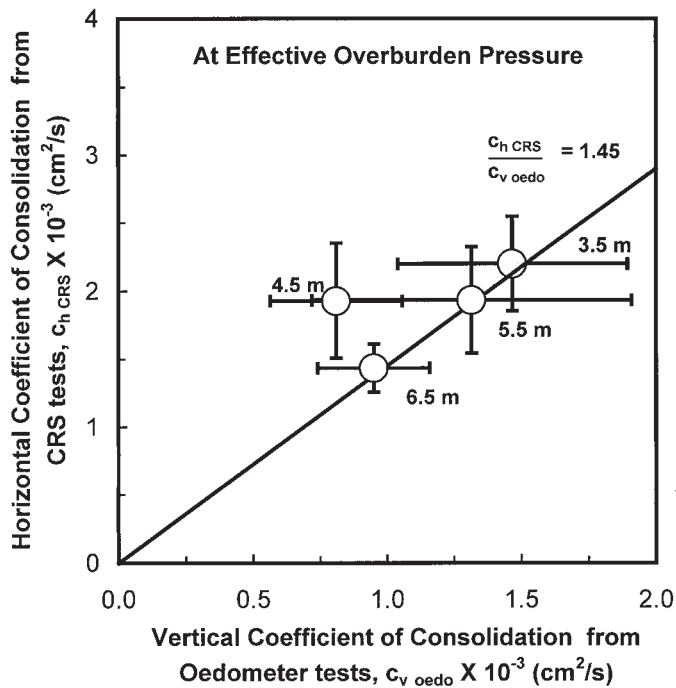


FIG. 17—Coefficients of consolidation in vertical and horizontal directions.

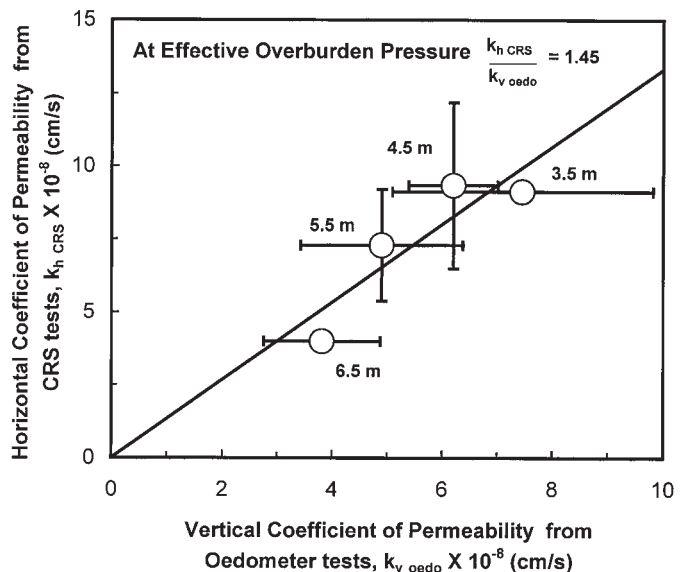


FIG. 19—Coefficients of permeability in vertical and horizontal directions.

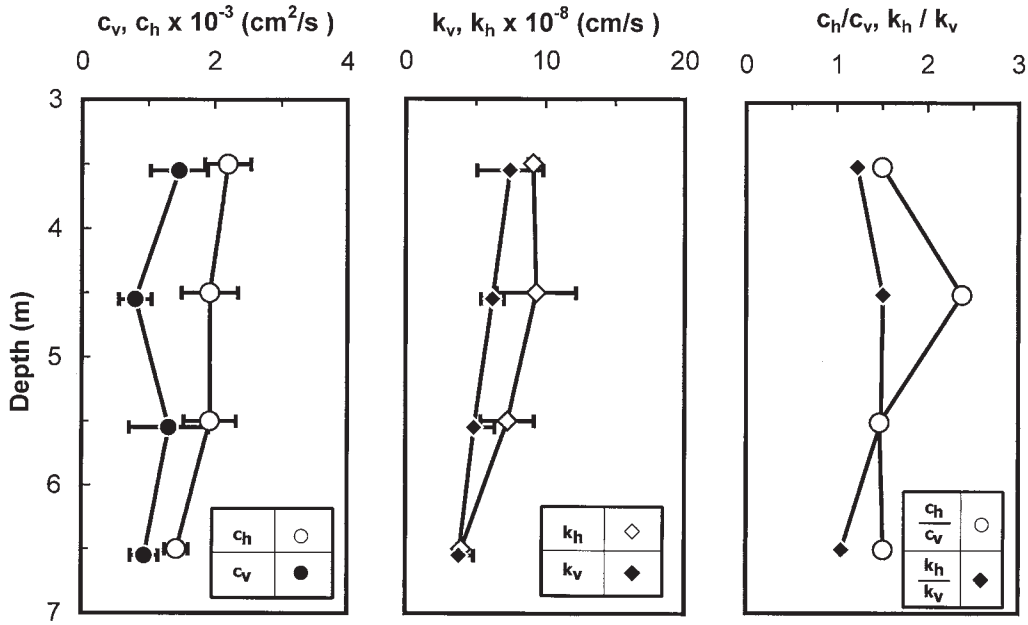


FIG. 20—Variations in coefficients of consolidation and permeability with depth.

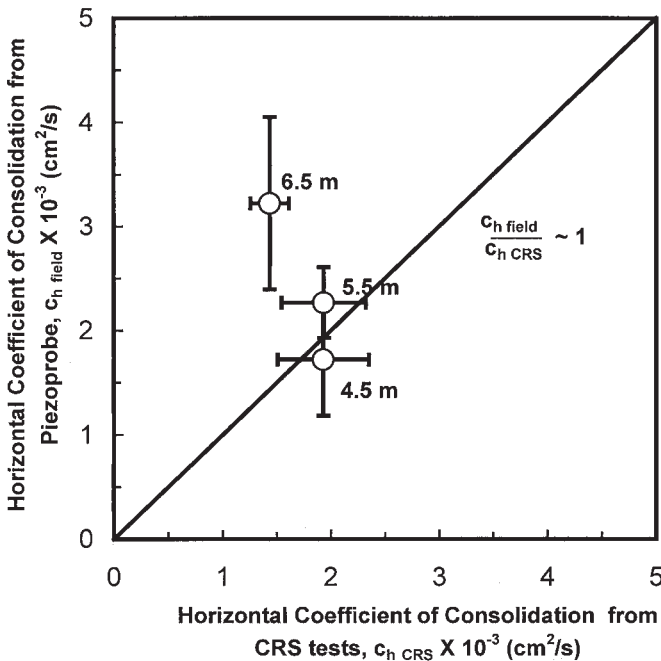


FIG. 21—Coefficients of consolidation from laboratory and field tests.

The profiles of coefficients of consolidation and permeability with depth are illustrated in Fig. 20.

Comparison of Coefficients of Consolidation from CRS and In-Situ Tests

The in-situ horizontal coefficients of consolidation were measured by means of dissipation tests (1994). A piezoprobe with a porous filter located just behind the cone measured pore pressure dissipation with time at various depths. Based on the dissipation curves, the in-situ horizontal coefficients of consolidation were es-

timated. Figure 21 shows a plot of c_h obtained from field dissipation curves versus those obtained from laboratory CRS tests, indicating good agreement except for the results at a depth of 6.5 m; the discrepancy is caused by variation in soil properties with presence of sand seams.

Conclusions

This research work concentrates on the determination of the horizontal coefficient of permeability, the horizontal coefficient of consolidation, and consolidation characteristics of soft Bangkok clay by using a new CRS consolidometer with radial drainage. Based on the results, the following conclusions can be made:

1. The measured ratios of u_a/u_b are in good agreement with those calculated from Barron's theory.
2. The horizontal coefficients of permeability and consolidation obtained from CRS test are independent of strain rate.
3. The preconsolidation pressures obtained by the new proposed method agree well with those obtained from the Casagrande method.
4. The strain rate is linearly proportional to the term γ as function of c_h , specimen radius, and pore pressure ratio.
5. Based on the results obtained from the CRS and oedometer tests, it can be concluded that secondary compression occurs during primary consolidation, indicating that Hypothesis B (Ladd et al. 1977) is valid for soft Bangkok clay.
6. The CRS compression curves at a strain rate of $1 \times 10^{-6}/s$ agree with those obtained from conventional oedometer tests. Hence, the CRS test at this strain rate can be used for routine testing on Bangkok clay.
7. The ratios of k_h/k_v and c_h/c_v at effective overburden stress from laboratory test results are about 1.45, indicating that Bangkok clay is anisotropic.
8. The horizontal coefficients of consolidation from field piezoprobe tests are in good agreement with the results from laboratory CRS tests.

Acknowledgments

The authors acknowledge technical assistance and review provided by friends from various universities, including Professor Hansbo, Professor Thomas Sheahan from Northeastern University, and Dr. Z. C. Moh from Moh and Associates Inc. for reviewing the draft and providing valuable comments. They are indebted to Mr. Tangthansup Burut for preparing the final manuscript.

References

- Barron, R. A., 1948, "Consolidation of Fine-Grained Soils by Drain Wells," *Transactions of ASCE*, Vol. 113, pp. 718–754.
- Butterfield, R., 1979, "A Natural Compression Law for Soils (An Advance on e -log p)," Technical Note, *Geotechnique*, Vol. 24, No. 4, pp. 469–480.
- Casagrande, A., 1936, "The Determination of the Preconsolidation Load and Its Practical Significance," *Proceedings of the 1st IC-SMFE*, Cambridge, MA, Vol. 3, pp. 60–64.
- Janbu, N. and Senneset, K., 1979, "Interpretation Procedures for Obtaining Soil Deformation Parameters," *Proceedings of the 7th ESCMFE*, Brighton, Vol. 1, pp. 185–188.
- Juirnarongrit, T., 1996, "Constant Rate of Strain of Consolidation Test with Radial Drainage," Master Thesis No. GE-95-14, Asian Institute of Technology, Bangkok, Thailand.
- Ladd, C. C., Foott, R., Ishihara, K., Schlosser, F., and Poulos, H. G., 1977, "Stress Deformation and Strength Characteristic SOA Report," *Proceedings of the Ninth International Conference of Soil Mechanics and Foundations Engineering*, Tokyo, Vol.2, pp. 421–494.
- Leroueil, S., 1988, "Recent Developments in Consolidation of Natural Clays," Tenth Canadian Geotechnical Colloquium, *Canadian Geotechnical Journal*, Vol. 25, pp. 85–107.
- Nesarajah, S., 1994, "Dissipation Testing on Bangkok Clay," Master Thesis No. GT-93-14, Asian Institute of Technology, Bangkok, Thailand.
- Rowe, P. W. and Barden, L., 1966, "A New Consolidation Cell," *Geotechnique*, Vol. 16, No. 2, pp. 162–170.
- Schmertmann, J. M., 1955, "The Undisturbed Consolidation of Clay," *Transactions of ASCE*, Vol. 120, pp. 1201–1233.
- Tavenas, F. Des Rosiers, J.-P., Leroueil, S., LaRochelle, P., and Roy, M., 1979, "The Use of Strain Energy as a Yield and Creep Criterion for Lightly Overconsolidated Clays," *Geotechnique*, Vol. 29, No. 3, pp. 285–303.